

Pressure Gradients on a Barred Beach

William Boylston

Advised by Takayuki Suzuki, Sungwon Shin, Daniel T. Cox

Oregon State University, Summer REU 2004

Abstract: Four wave cases were run in a 2-D wave flume with a barred beach cross-shore profile to provide data on how bars affect cross-shore pressure gradients. An array of four pressure transducers was used to calculate the exceedance probability of the pressure gradient at eight cross-shore locations. The data shows that pressure gradients increase approaching the bar from off shore, and decrease once the bar has been passed. Also, based on a critical value of the pressure gradient defined by Madsen (1974), sediment suspension due to horizontal pressure gradients can be assumed to occur approximately every hundred waves. A tendency for offshore gradients to exceed onshore gradients makes offshore movement of sediment likely.

Introduction:

In coastal processes, sediment instability is a conundrum. As waves shoal and break, they produce a variety of forces that result in the loosening of sediment. Unfortunately, due to the highly random nature of these constituent forces it is difficult to separate the effects of one force from another. Yet, because sediment instability is a fundamental step for sediment transport, understanding and grasping any new information pertaining to it is worthwhile.

One type of force acting on sediment results from pressure gradients that are due to the free surface fluctuations of waves. Hsu and Ariyaratnam (2000) suggest that pore-water pressure gradients within the sediment of the swash zone are responsible for accretion or erosion from the beach surface. This is an example of how water pushing through the sand bed can have formative effects on the shore. Sakai and Gotoh (1996) found that the amplitude of the change in vertical water pressure is responsible for rippling the sand bed and creating an asymmetrical geometry. Under the low-pressure troughs of waves, pore-water pressure vertically lifts sediment, resulting in instability. The ability of pressure gradients to affect the sand bottom is documented. However, to experimentally observe instability without a sediment bed, critical values of pressure gradients, as well as their directions, must be known.

With the purpose of defining when and how pressure gradients most significantly create instability, Madsen (1974) proposed that horizontal pressure gradients are greater in magnitude than vertical, and therefore more responsible for exhibited instability. Further, using an analysis of forces at work within sand beds, the critical value needed for

sand bed instability was concluded to be $\Delta P^* = -\frac{dp}{dx} \frac{1}{\rho g} = 0.5$. This is a normalized

pressure gradient, where ρ is the density of water, and g is the acceleration of gravity. A later analysis by Cox, *et al.* (1991) suggested a critical value of 0.4. These critical values

can be used to infer upon lab data whether sediment instability will occur under an experiment's conditions.

Submerged sand bars are known to migrate in the onshore direction under the influence of ocean waves not of storm related origins. Arntsen, et al. (2000), found that for steeper slopes, such as the offshore face of sand bars, the magnitude of pressure gradients increases. As slope increases, decreasing the water depth, there is less water present to cushion the energy of a breaking wave. Also, a narrower band of sand bottom is presented for the wave to transfer its energy to. Greater energy incident upon a smaller area leads to a sharper change in pressure horizontally. This leads to a greater likelihood of sediment suspension, and in turn, greater sediment transport. Consequently, horizontal pressure gradients, always present with wave action, may play a key role in the migration of sand bars.

Outline of Experiment:

Using a 2D wave flume 104 meters in length and 3.7 meters wide, waves were run at the barred cross-shore profile shown in fig1. Data was collected at eight cross-shore locations. The locations were chosen to provide ample data about how pressure gradients along the sand bed behave as waves propagate along barred beaches. Each position is marked in fig. 1. The water depth and distance from the wave maker, for each position, are given in table 1. Pressure was measured using an array of four pressure transducers,

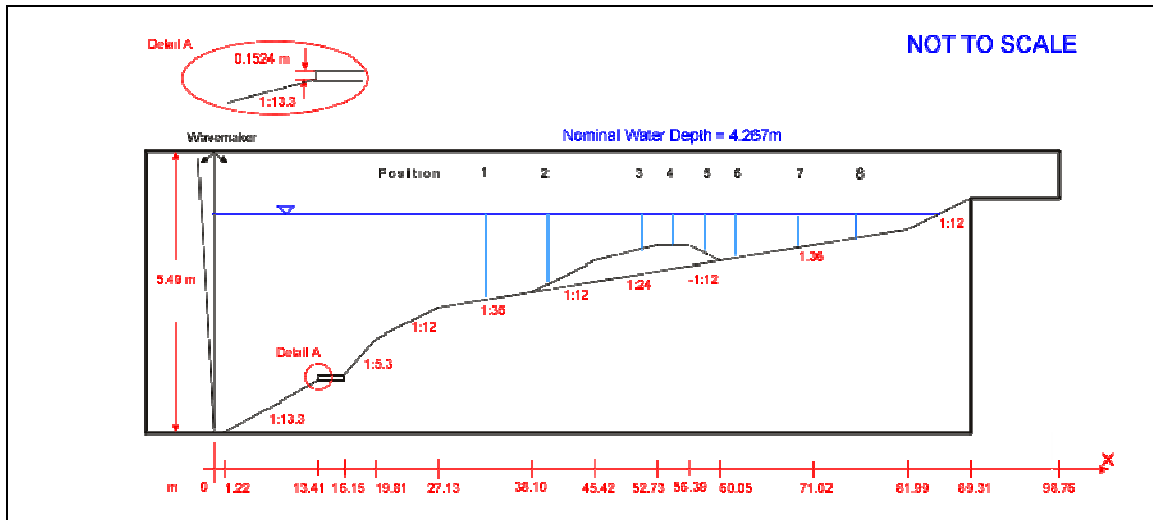


Figure 1: Cross-Shore Bathymetry and Positions of Data Collection

Table 1: Water Depth and Distance from the Wave Maker

Position	h(m)	x(m)
1	1.75	32.61
2	1.46	39.93
3	.774	50.90
4	.707	54.56
5	.851	58.22
6	.957	61.87
7	.756	69.19
8	.543	76.50

linearly placed in 3cm increments. The transducer array, wave gauges, and ADVs, were attached to a movable cart that rests on the walls of the wave flume. At each measurement location, a mobile frame lowered the transducer array until it rested on the tank's bottom. A swivel was built into the transducer array, enabling its angle to match the wave tank's bathymetry at all locations cross-shore.

Wave height measurements were taken from three capacitor type wave gauges. Two were 30.7cm onshore and offshore, respectively, of the pressure transducer array. The gauge lay out is shown in fig. 2. For measurement position 8, this arrangement was altered due to limitations of cable lengths. Wave gauge 6 was moved out to 34.29cm, and wave gauge 7 was brought in to 17.45cm. Also, for measurement locations 1 and 2, the separation distance for each gauge was 30.5cm, a loss of 2mm.

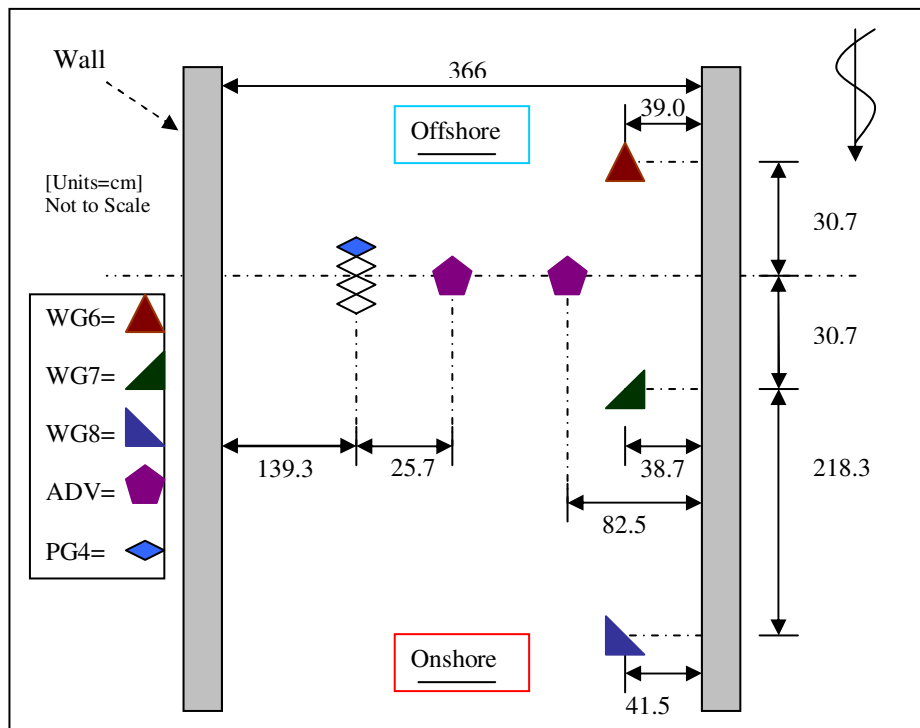


Figure 2: Physical Arrangement of Data Collection Equipment Relative to the Walls of the Wave Flume

Four wave cases were run at each location. One regular wave case, $H=0.6\text{m}$ $T=4.0\text{s}$, was chosen to show the effects of waves breaking on the bar. An irregular wave case of similar wave height and period was selected to show probability of sediment instability under naturalistic conditions of ocean waves breaking on a bar. The final two regular wave cases were to further develop an understanding of how gradients behave in various wave conditions. Each wave cases target wave height, peak period, and duration, are shown in table 2. These waves are large relative to the size of the bar and flume.

Table 2: Data for each wave case

Case	H(m)	T(s)	Wave Type	Duration(s)
1	0.6	4.0	Regular	700
2	0.6	2.7	Regular	700
3	0.5	5.0	Regular	700
4	0.6	4.0	Irregular	1200

All voltage outputs were collected by a data acquisition program at a 50Hz sampling frequency. To calibrate this data, voltage outputs of all gauges and transducers were measured at various submerged depths. A linear fit was put to the calibration data, and its slope relates volts to meters. The magnitude of the slope became each gauges calibration number. Upon making a product of each voltage reading and the respective gauge's calibration number, the data became suitable for analysis.

Analysis:

For the regular wave cases run, wave height increases as waves approach the bar. This increase in wave height, accompanied by a narrowing of the wave's peak, creates measurably increased pressure gradients as one approaches the bar from offshore. After waves break on the bar, or continue into the deeper water onshore of the bar, the pressure gradient's magnitude recedes, and does not increase again until the waves shoals on the shoreline. This increase over the bar, and subsequent decrease, can be seen in fig. 3. Figure 3 shows cross-shore progress of the phase averaged free surface fluctuation, and the phase averaged pressure gradient. In this figure, offshore pressure gradients are of note. Just as the magnitude of the positive pressure gradient increases over the bar, the negative, or offshore, pressure gradient increases. These peaks of on and offshore pressure gradient occur before and after the peaks of passing waves. The pressure gradient in fig. 3 was calculated using the data of four pressure transducers to approximate the gradient about the center of the array. Wave gauge six was taken to represent the free surface for phase averaging, with the free surface fluctuation, η , normalized by the deep-water significant wave height, H_0 . $\eta^* = \frac{\eta}{H_0}$.

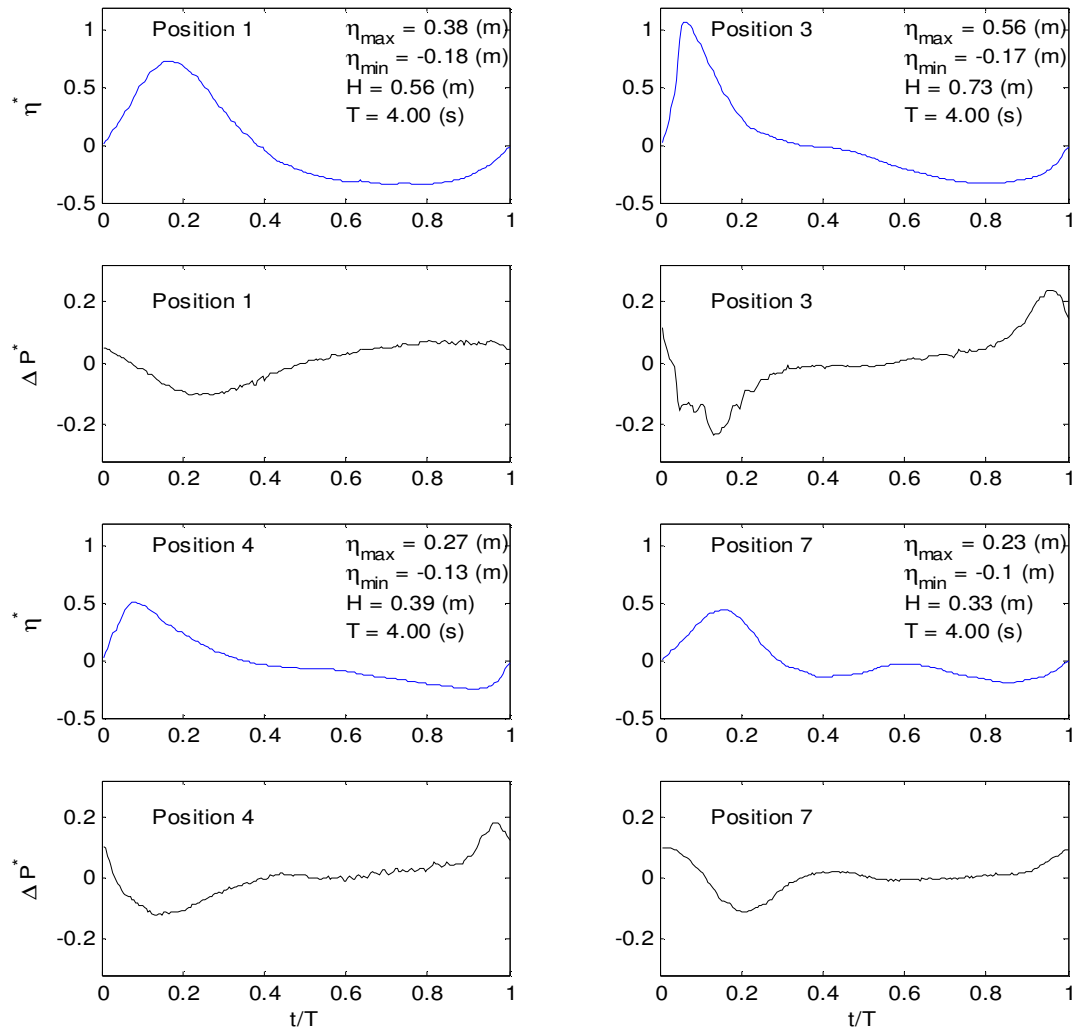


Figure 3: Phase Average for Free Surface Fluctuations and Pressure Gradient at Four Cross-Shore Locations

Various methods were available for calculating pressure gradients, (dp/dx), of the data.

1. $-\frac{Pg1 - Pg4}{0.09}$: This is a linear approximation of the gradient made by taking the difference between pressure gauge 1 (onshore) and pressure gauge 4, and dividing it by the 0.09m distance between the two pressure gauges.
2. $-\frac{Pg2 - Pg3}{0.03}$: This is similar to 1, but involves the two central gauges that are positioned only 3cm apart.
3. $-\frac{Pg4 - 27Pg3 + 27Pg2 - Pg1}{24 * 0.03}$: This fits a curve to the four points and uses the space between each gauge, 0.03m, as dx .

Lines calculated using methods one and four are relatively smooth. Methods 2 and 3 produce noisier lines, one example being ΔP^* of the irregular wave in fig. 4.

Figure 4 shows waves over the bar for the irregular wave case. The shape of the free surface is very similar to the pressure at tank bottom. In addition, the pressure gradient peaks before the wave crest, and experiences a minimum after the crest passes.

The noise exhibited in pressure gradient values is likely an artifact of the data acquisition system. Method 1 has a value of $dx=0.09m$, and the change in pressure over this distance is large enough to be adequately expressed by the data acquisition system. However, method 2 involves pressures that are so similar the difference becomes obscured by bit noise. That is, the signal change is so small that it has to be rounded off to discrete levels, and results in a stair-stepped figure. Method 3 has similar stair stepping, but the effects of two close pressure gauges are tempered by inclusion of notably different outlying pressure gauges.

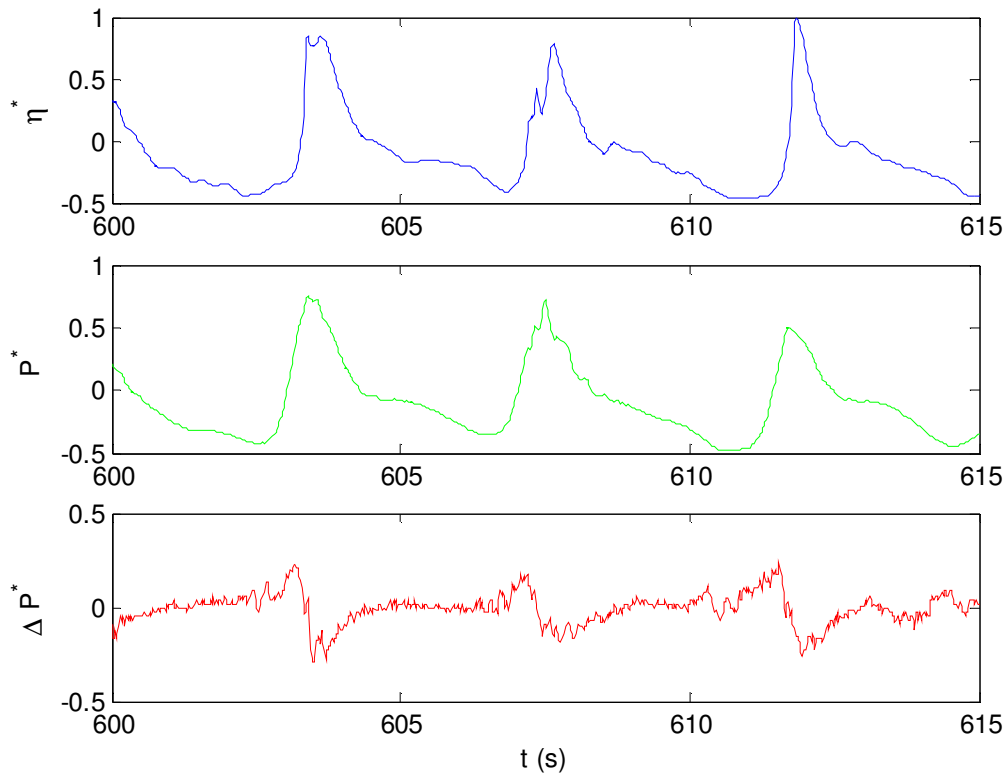


Figure 4: Free Surface, Normalized Pressure $P^* = \frac{P}{\rho g H_0}$, and dp/dx for Wave Case 4 at Position 4.

Using data from the irregular wave case, exceedance probability was calculated for the magnitude of the pressure gradient at all cross-shore locations. C is used in this paper to represent the gradient in the positive onshore direction. $C_{1/3}$ is calculated by taking the largest positive gradient value from each wave, and then averaging the highest third of these maximum gradient values. R represents dp/dx in the negative offshore direction, and $R_{1/3}$ differs from $C_{1/3}$ only in its use of the largest negative gradients, rather than positive. Probability of exceedance for C and R were calculated using methods one, two, and three of finding dp/dx . This is shown in fig. 5.

Differences in calculation methods for dp/dx affect the exceedance probability measured. For method two, because the curve of dp/dx has discrete levels along it, the peak of each wave also has notably discrete levels. The bit size is so large compared to the data's fluctuation that there are very few levels available as values of ΔP^* .

Accordingly, the values of ΔP^* appear as concentrated groups in fig. 5.

The method with $dx=9\text{cm}$ is smoother, and less obscured by noise. Nevertheless, the values of ΔP^* calculated and shown in fig. 5 are noticeably lower than those made with methods using smaller dx . Therefore, for our wave case, a separation of nine centimeters is often unable to measure the peak pressure gradient of waves. The two points of data collection are far enough apart, relative to wavelength, that short lived large gradient events are smoothed over. Events with dx less than 9cm are incapable of affecting both pressure transducers simultaneously, and do not appear in full. This means a wide separation acts similar to a low pass filter. Spikes of large magnitude are lost, and a more consistent base of low values remains.

Method 3 records large gradient events and is capable of a broad range of values. This method uses a separation of three centimeters, allowing it to record and express more brief pressure gradient fluctuations. Due to its finer ability to record information, short-lived high gradient events appear in the data. Also, because the two outlying gauges apply averaging effects to the more weighted central gauges, bit noise is not as pronounced. This results in a smooth distribution of gradient maximums within the exceedance probability figure. This method is used for calculating the cross-shore exceedance probability shown fig. 6 & 7.

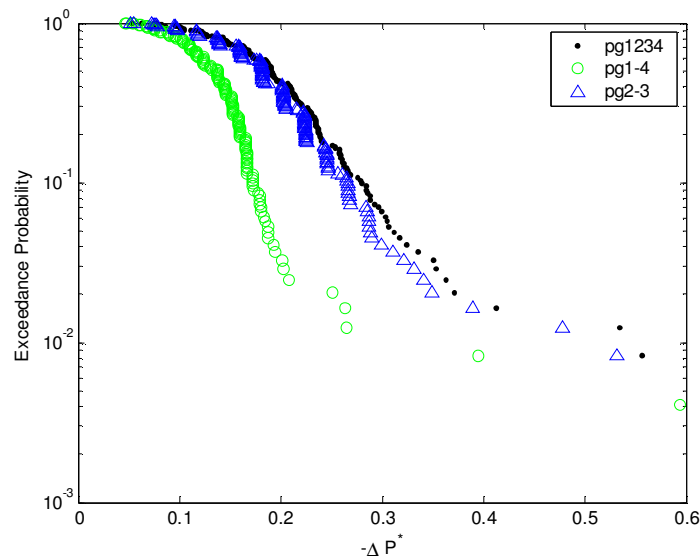


Figure 5: Exceedance Probability of the Pressure Gradient in the Offshore direction for Three Methods of Calculating ΔP^* .

Figures 6 & 7 show that the probability for large values of ΔP^* is highest over the bar. As waves propagate onshore, the number of wave events with relatively large magnitude increases, and those large magnitudes become more probable. For many

positions, it is probable to have an offshore gradient that is larger than its onshore partner is. This is visible when comparing the $C_{1/3}$ and $R_{1/3}$ values for each position.

In the P_E graphs for positions 4 and 5, there are a few outlying points of high magnitude, both on and off shore. These points tended to occur in wave troughs, and they do not lay on the Rayleigh curve. They also tend to result from large variations in all four transducer readings, rather than from one transducer greatly diverging from the other three. Further, the duration of these peaks often encompassed multiple time samples. They are not often spikes containing only one data point. Also, it must be noted that the data for position three stops at time=568s. Pressure gauge 2 began behaving erratically at that point, but data prior to t=568s appears unaffected.

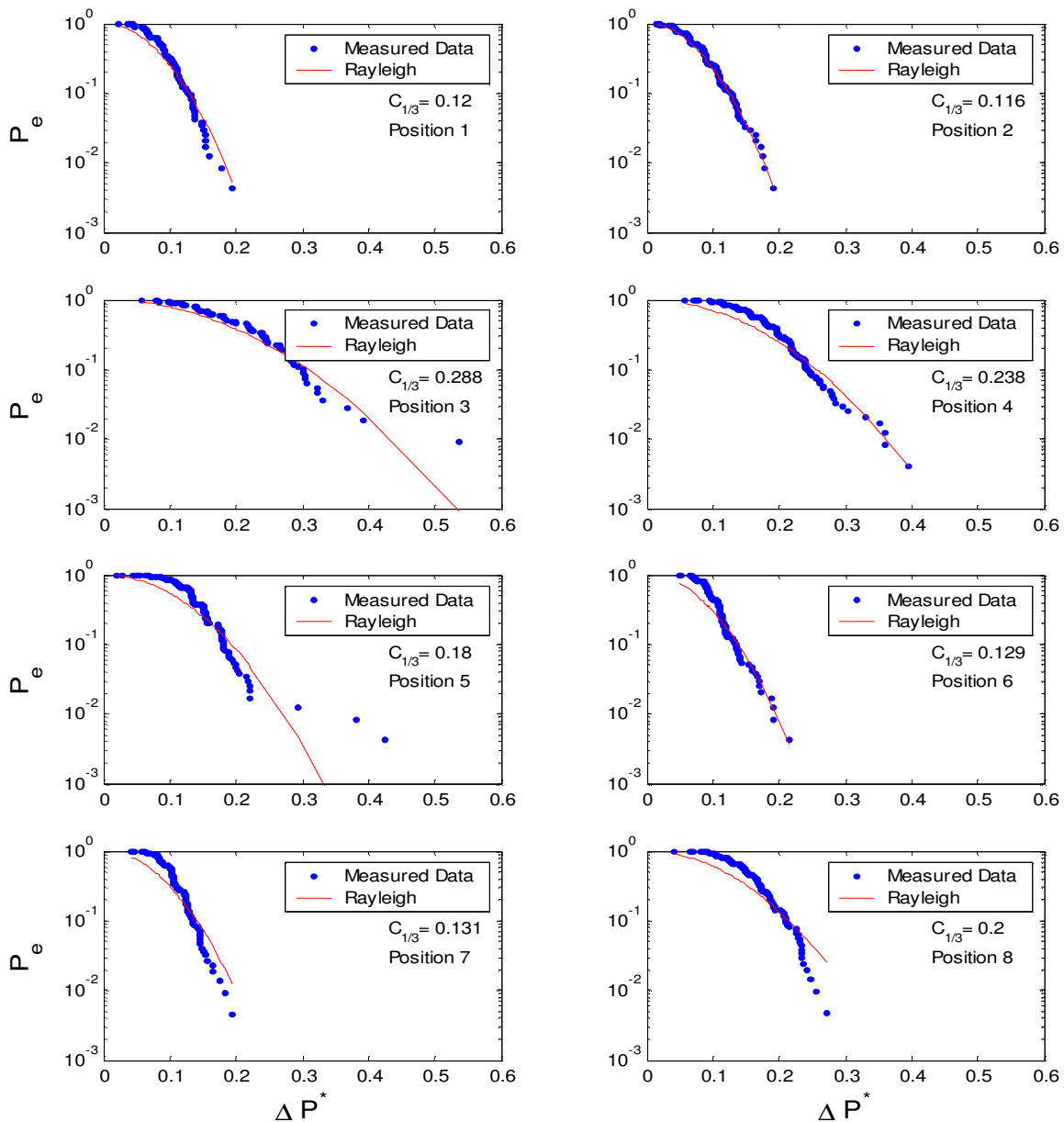


Figure 6: Exceedance Probability for Pressure Gradients in the Onshore Direction at Eight Cross-Shore Locations

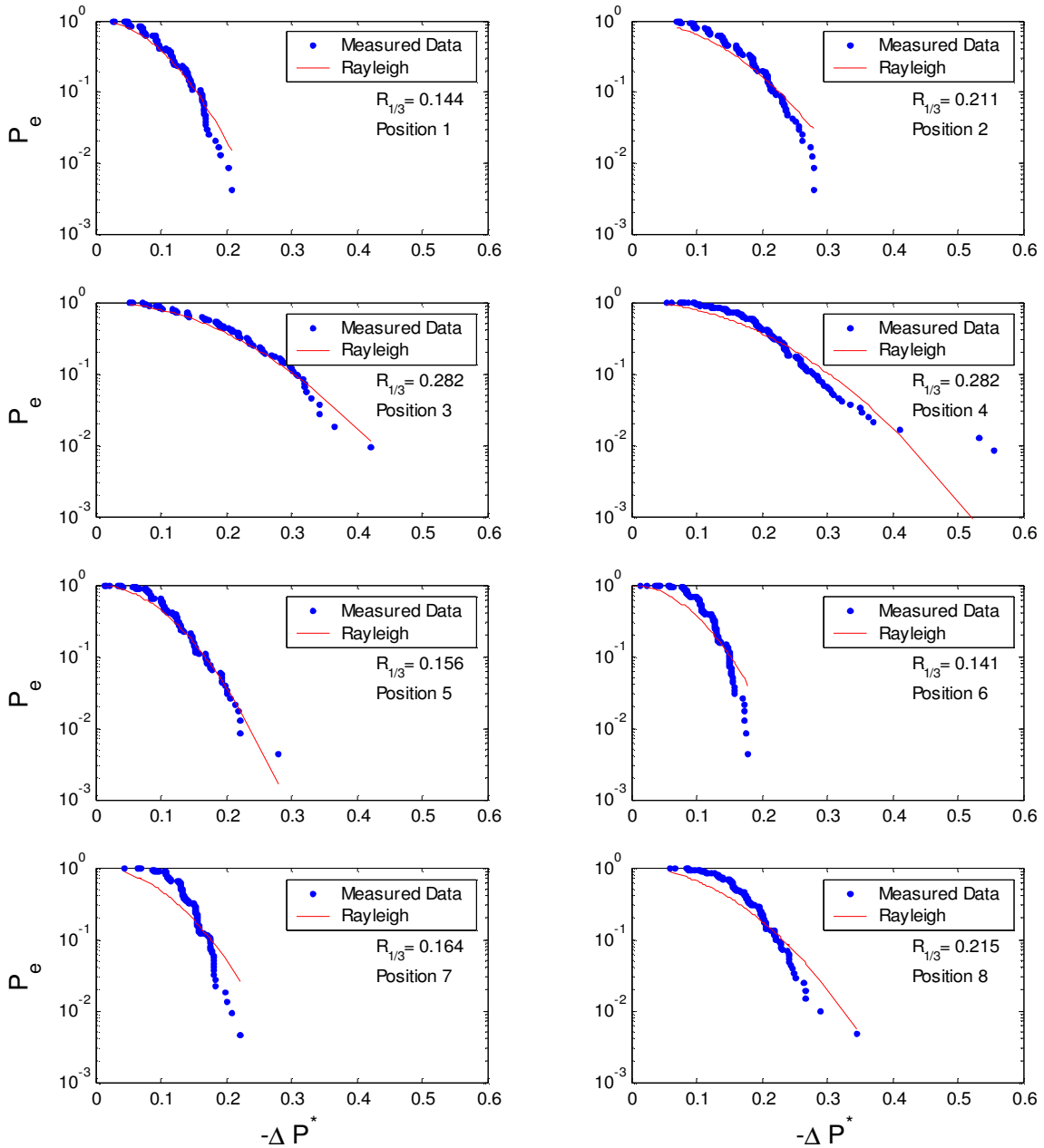


Figure 7: Exceedance Probability for Pressure Gradients in the Offshore Direction at Eight Cross-Shore Locations

Discussion:

Four wave cases were run at a barred beach with the results that pressure gradients increased over the bar, dipped after, and increased slightly again when the waves shoaled and broke on the shore. To understand this better, a reliable method of calculating dp/dx must be found. Upon that, more qualified and reliable inference upon the physical situation can be made. Because data from two transducers with a 3cm separation is overly quantized, it does not represent the waves well. Yet, if transducers are at a larger separation, data fluctuations of short length are poorly recorded. Due to its ability to

capture information, and represent it well, the method with four transducers is the best reference for behavior of our experimental wave cases.

The highest probability of sediment suspension occurs over the bar. Based on the critical value of $\Delta P^* = 0.4$, there is approximately a 1% chance of sediment being suspended over the bar by either an onshore or offshore pressure gradient. This could be large enough to have a noticeable effect on long-term sediment transport. Additionally, it is most likely that the offshore gradient is larger than the onshore one, for most positions. Under such conditions, sediment should be moving off shore. This is consistent with natural conditions where relatively large waves cause the off shore migration of sand bars.

Acknowledgements:

Takayuki Suzuki, Sungwon Shin, and Dr. Cox, for aiding and advising

Funding for this Research Experience for Undergraduates (REU) site was provided by the National Science Foundation (EEC-0244205). The O.H. Hinsdale Wave Research Laboratory was partially supported by the National Science Foundation as part of the George E. Brown Network for Earthquake Engineering Simulation (NEES) program (CMS-0086571).

References:

- Cox, D.T., Kobayashi, N., and Mase, H., 1991, "Effects of Fluid Accelerations on Sediment Transport in Surf Zones", *Coastal Sediments*, 447-461.
- Madsen, O.S., 1974, "Stability of a Sand Bed Under Breaking Waves", *Coastal Engineering*, 776-794.
- Hsu, J.R., and Ariyaratnam, J., 2000, "Pressure Fluctuations and a Mechanism of Sediment Suspension in Swash Zone", *Coastal Engineering*, 610-623.
- Sakai, T., and Gotoh, H., 1996, "Effects of Wave-Induced-Pressure on Seabed Configuration", *Coastal Engineering*, 3155-3168.
- Arntsen, O.A., *et al.*, 2000, "Wave kinematics and wave bottom pressures in the surf zone", *Coastal Engineering*, 1008-1021.